Characterization of Fluid Distributions in Porous Media by NMR Techniques

Hsie-Keng Liaw, Raghavendra Kulkarni, Songhua Chen, and A. Ted Watson
Dept. of Chemical Engineering, Texas A&M University, College Station, TX 77843

Nuclear magnetic resonance (NMR) spin-lattice relaxation measurements are used to investigate pore structures and fluid phase distributions in porous media. A new method for estimating relaxation time distribution functions from measured relaxation data is presented using a B-spline basis to represent the distribution function and Tikhonov regularization to stabilize the estimation problem. Surface relaxivity, which is required to convert relaxation time distributions to pore-size distributions or fluid phase distributions at partial saturations, is determined using pore volume-to-surface-area ratios estimated by NMR diffusion measurements. This approach was validated by analyzing certain model porous media with known pore volume-to-surface-area ratios. The method is demonstrated by determining pore-size and fluid phase distributions of sandstone and carbonate samples, as well as by comparing the pore-size distributions of chalk samples obtained by this methodology with those estimated by mercury porosimetry.

Introduction

The characterization of pore structures and fluid phase distributions in porous media is of fundamental importance for accurate evaluation of reservoir resources and petroleum recovery as well as for environmental remediation and many chemical engineering processes. Although there are a number of conventional methods that attempt to characterize pore structures in porous media, they are subject to serious limitations. For example, mercury porosimetry tends to reflect pore throat sizes, rather than pore sizes. Furthermore, this method is based on the bundle of capillary tubes model for data interpretation. That model is known to be a poor representation for most porous media. Nitrogen adsorption requires pore-shape assumptions and can only explore a limited pore-size range. Thin-section analysis can provide structural information. However, it does not observe actual three-dimensional structures, it tends to miss small pores, and it is difficult to sample reasonably large numbers of pores. Moreover, all those methods are destructive and are not suitable for exploring multiphase situations.

The nuclear magnetic resonance (NMR) spin-lattice relaxation measurement does not have the disadvantages just cited. Furthermore, it can be used to determine information about fluid phase distributions in multiphase situations. It can probe a wide range of pore sizes and does not require pore-shape assumptions. The use of this approach is based on the observation that molecules in the immediate vicinity of pore boundaries have enhanced rates of relaxation. In the fast-exchange limit (Brownstein and Tarr, 1977), the relaxation rate exhibited by a single pore is directly related to the product of the surface relaxivity and the pore surface-to-volume ratio. The observed NMR signals are a convolution of the relaxations of fluid in the various pores throughout the observed system.

Suitable interpretation of NMR relaxation data can provide an estimate of pore-size distribution for situations in which a porous medium is fully saturated with the observed fluid phase. Information about the fluid phase distributions can be obtained in situations for which the media contain multiple fluid phases (Straley et al., 1991; Chen et al., 1993a; Borgia et al., 1994; Chen et al., 1994). In this work, a new method for recovering pore volume-to-surface-area distributions from measured spin-lattice relaxation data is developed. Its use to characterize pore structures and fluid phase distributions for media containing two immiscible fluid phases is demonstrated.

The estimation of pore volume-to-surface-area distributions from relaxation data involves the solution of a Fredholm integral equation of the first kind. This is known to be an ill-posed problem (Wahba, 1977; Groetsch, 1984), so suitable solution is critical to the success of the method. A new

method is presented here for solution of that integral equation. It features the use of B-splines to represent the unknown function and Tikhonov regularization to stabilize the estimation problem. In addition, linear inequality constraints are incorporated in order to ensure nonnegativity of the estimated distribution.

A convenient method for estimating the surface relaxivity is provided. This has been problematic for the interpretation of relaxation data. Previous methods have been based on data obtained using mercury injection or thin-section analysis (Brown et al., 1982; Gallegos and Smith, 1988; Kenyon et al., 1989; Howard and Spinler, 1993), and thus suffer from limitations previously cited. This method is based on the use of NMR diffusion measurements to estimate the pore volume-to-surface-area ratios. With these experiments, the entire sample is observed, so a more realistic estimate of surface relaxivity can be expected. This approach is validated by analyzing certain model porous media with known pore volume-to-surface-area ratios.

Theory

NMR spin-lattice relaxation measurements of pore volume-to-surface-area distribution

The magnetization evolution of spin-lattice relaxation for fluid in the bulk phase, probed by the inversion-recovery sequence, can be represented as

$$M(t) = M_0\left[1-2\exp\left(-\frac{t}{T_1}\right)\right], \tag{1}$$

where $M(t)$ is the magnetization at recovery time t and M_0 is the intrinsic magnetization. Zimmerman and Brittin (1957) proposed that at the fast-exchange limit, the spin-lattice relaxation for fluid confined in a pore can be represented as a single-exponential decay. This is due to the fact that the bulk and surface phase relaxation effects are coupled together under the fast-exchange limit. The relaxation time T_1 for fluid confined in a pore is given by (Brownstein and Tarr, 1977)

$$\frac{1}{T_1} = \left(1-\frac{\eta S}{V}\right)\frac{1}{T_{1b}} + \frac{\eta S}{V}\frac{1}{T_{1s}} \simeq \frac{1}{T_{1b}} + \frac{\eta}{T_{1s}}\frac{S}{V} = \frac{1}{T_{1b}} + \frac{1}{\tau_1}, \tag{2}$$

where T_{1b} is the relaxation time in the bulk fluid phase, T_{1s} is the relaxation time in a surface layer adjacent to the pore boundaries, η is the thickness of the surface layer, and τ_1 is a characteristic relaxation time excluding the bulk phase relaxation effect. It is expected that T_{1s} is much smaller than T_{1b} because of the much stronger surface interactions between pore boundaries and fluid molecules compared with the interactions among fluid molecules. The surface relaxivity ρ, which represents the interaction strength between fluid and pore boundaries, is defined as $\rho = \eta/T_{1s}$. Surface relaxivity is usually treated as a constant for simplification, although it is probably not uniform throughout the porous system. The characteristic relaxation time τ_1, which is dependent on pore structures and surface relaxivity, is directly proportional to the pore volume-to-surface-area ratio V/S.

Spin-lattice relaxation measurements for fluid confined in a porous medium represent a distribution of T_1 values, as opposed to a single T_1 value as exhibited by bulk fluid or fluid confined in a single pore. This is due to a distribution of pore sizes within the porous system. If the bulk phase relaxation effect is assumed to be negligible, T_1 and the corresponding distribution function $P(T_1)$ are proportional to the pore volume-to-surface-area ratio V/S and its distribution function $P(V/S)$, respectively. However, this assumption might not be valid for the fluid confined in large pores (in other words, when T_1 is not significantly less than T_{1b}). Therefore, the distribution function $P(V/S)$ is best determined from the distribution function of τ_1, $P(\tau_1)$, instead of from $P(T_1)$.

The observed magnetization at recovery time t_i in a porous system is given by the fluid confined in all of the pores, which can be represented as

$$\frac{M^{\text{obs}}(t_i)}{M_0} = \int_{\tau_{1\,\min}}^{\tau_{1\,\max}} P(\tau_1)\left\{1-2\exp\left[-t_i\left(\frac{1}{T_{1b}}+\frac{1}{\tau_1}\right)\right]\right\}d\tau_1 + \epsilon_i, \quad i = 1, 2, \ldots, n_{\text{obs}}, \tag{3}$$

where n_{obs} is the number of observations, ϵ_i is the measurement error, $P(\tau_1)$ is the normalized distribution function of τ_1, and

$$\int_{\tau_{1\,\min}}^{\tau_{1\,\max}} P(\tau_1)\, d\tau_1 = 1. \tag{4}$$

It is observed that τ_1 and $P(\tau_1)$ can be converted to V/S and $P(V/S)$ based on the relationship in Eq. 2, as long as the surface relaxivity is determined. The average pore volume-to-surface-area ratios of the tested samples were determined from NMR diffusion measurements at short diffusion times, then compared with the average τ_1 to estimate the values of surface relaxivity. This is described in more detail below. We will refer to the pore volume-to-surface-area ratio V/S and its distribution function $P(V/S)$ for the fully water-saturated sample as pore size and pore-size distribution, hereafter. The assumption involved in converting $P(\tau_1)$ to $P(V/S)$ is that the interpore coupling is negligible, which might not be valid for very small pores.

Interpretation of spin-lattice relaxation data

The distribution function $P(\tau_1)$ can be estimated from the relaxation data measured by the inversion-recovery sequence using Eq. 3, which relates the distribution function to the measured data. That equation can be expressed as

$$y_i^{\text{obs}} = \int_{\tau_{1\,\min}}^{\tau_{1\,\max}} P(\tau_1)k_i(\tau_1)\, d\tau_1 + \epsilon_i, \quad i = 1, 2, \ldots, n_{\text{obs}}. \tag{5}$$

Equation 5 is a Fredholm integral equation of the first kind, and the recovery of the distribution function from the observations is known to be an ill-posed problem. In particular,

note that the value of the integral depends on the entire distribution function within $(\tau_{1\min},\tau_{1\max})$, but only a finite number of data are available to recover that function. It is known that Tikhonov regularization (Wahba, 1977; Merz, 1980, Groetsch, 1984) can provide stable solutions of this ill-posed problem. This is discussed further below.

A finite-dimensional representation of the unknown function $P(\tau_1)$ is required. We expect relaxation time and pore-size distributions to be best represented as continuous functions. Consequently, we propose to employ B-splines, which can accurately approximate any smooth function (Schumaker, 1981), for the representation of the distribution function. The distribution function is thus given by

$$P(\tau_1) = \sum_{j=1}^{n} c_j B_j^m(\tau_1), \tag{6}$$

where $B_j^m(\tau_1)$ is the mth order B-spline function and c_j its corresponding coefficient. A sufficiently large dimension of the spline, n, is used so that the estimation of the distribution function is largely uninfluenced by the number and position of the knots. Previous approaches for estimating pore-size distributions from relaxation data have represented the unknown distribution function as a series of delta functions (e.g., Kenyon et al., 1989; Whittall et al., 1991; Howard and Spinler, 1993). The estimated functions so obtained are not continuous. Furthermore, continuous representations subsequently constructed for further manipulations of the distributions may not be consistent with the measured data, unlike the representation provided by the B-splines.

Assuming that measurement errors are independent and identically distributed [other assumptions can be accommodated within the norm used to relate the differences in observed and calculated values (Bard, 1974)], the problem can be posed as the determination of the distribution function that minimizes the following performance index:

$$J[\lambda,P(\tau_1)] = \|Y^{\text{obs}} - Y^{\text{cal}}\|^2 + \lambda \int_{\tau_{1\min}}^{\tau_{1\max}} |\,\mathcal{L}P(\tau_1)|^2\, d\tau_1, \tag{7}$$

where y_i^{cal} is the integral term in Eq. 5 and $\mathcal{L}$ is the regularization operator. Since the distribution function is nonnegative, it is desirable to include the nonnegativity constraint:

$$P(\tau_1) \geq 0. \tag{8}$$

The overall smoothing is controlled through the selection of the regularization parameter λ. Most of the previous applications of regularization to this problem (e.g., Gallegos and Smith, 1988; Kenyon et al., 1989; Straley et al., 1991; Howard and Spinler, 1993) have taken the regularization operator $\mathcal{L}$ to be the identity. Excursions of the estimated function from the mean value are thus reduced, tending to a leveling of the estimated distribution. Here, we choose the second derivative as the regularizing operator. In this way, sharp changes in the estimated distribution function are attenuated. This regularization is more consistent with the representation of the unknown distribution as being relatively smooth.

Using Eqs. 5–8, the problem is thus the determination of the coefficients $\boldsymbol{C}$ that minimize

$$J(\lambda,\boldsymbol{C}) = \|\boldsymbol{Y}^{\text{obs}} - \boldsymbol{AC}\|^2 + \lambda\|\boldsymbol{LC}\|^2, \tag{9}$$

subject to the nonnegativity constraints:

$$c_j \geq 0, \qquad j = 1,2, \ldots, n, \tag{10}$$

where

$$\|\boldsymbol{LC}\|^2 = \sum_{j=1}^{n} (c_{j-1} - 2c_j + c_{j+1})^2 \tag{11}$$

and

$$a_{ij} = \int_{\tau_{1\min}}^{\tau_{1\max}} B_j^m(\tau_1) k_i(\tau_1)\, d\tau_1. \tag{12}$$

For a given value of the regularization parameter λ, this minimization problem is a linear least-squares problem with linear inequality constraints. The solution, which is global, can be found in a finite number of steps (Lawson and Hanson, 1974).

The final task is to select an appropriate value of the regularization parameter. A variety of methods have been put forth (see Hansen, 1992, for a recent review and analysis). We use a method for which we identify the largest value of λ that does not compromise the precision of the fit to the data. This method had been proposed by Yang and Watson (1991) to choose the appropriate value of Bayesian weighting parameter for estimating the relative permeability curves, and it will select similar values as the L-curve method described by Hansen (1992). A larger value of the regularization parameter tends to lead to an oversmoothed distribution that provides a less precise fit to the data. On the other hand, a smaller value tends to provide a solution that is not sufficiently smooth; that is, higher frequencies are represented in the solution than are required to reconcile the measured data.

NMR diffusion measurements of pore volume-to-surface-area ratio

The use of NMR diffusion techniques for exploring pore structures is based on the fact that the observed diffusivity depends on the time over which the diffusion motion is observed. The time-dependence is related to the pore structures. Thus, by analyzing the diffusion behavior and its time-dependence, one can obtain pore structure information. In the short diffusion time region, the diffusivity D varies with observation time t as (Mitra and Sen, 1992)

$$\frac{D(t)}{D_0} = 1 - \frac{4}{3l\sqrt{\pi}} \frac{S}{V} \sqrt{D_0 t} + O(D_0 t), \tag{13}$$

where l is the spatial dimension, D_0 is the bulk fluid diffusivity, and S/V is the pore surface-to-volume ratio. Mitra et al. (1993) demonstrated that the coefficient of $\sqrt{D_0 t}$ is independent of surface relaxivity, and thus S/V can be determined, regardless of the unknown surface relaxivity. At long diffusion times (Haus and Kehr, 1987),

$$\frac{D(t)}{D_0} = \frac{1}{\alpha} + \frac{\beta_1}{t} - \frac{\beta_2}{t^{3/2}}, \tag{14}$$

where α is the tortuosity and β_1 and β_2 are constants related to microscopic details.

In our approach for surface relaxivity, NMR diffusion measurements are conducted at a fixed short diffusion time by varying the magnitude of the applied gradient, g_a. A short diffusion time model based on Eq. 13 is used to represent the variation of magnetization with g_a. This model can be represented by a straight line in a semilog scale. The pore surface-to-volume ratio, which is proportional to the slope of this line, can thus be calculated and compared with the average relaxation time to determine the value of surface relaxivity. Hürlimann et al. (1994) conducted diffusion experiments at various diffusion times across short and long diffusion time regions and then used the two-point Padé approximate (Latour et al., 1993) for data fitting to estimate S/V, which was compared with the average spin-lattice relaxation rate to determine the surface relaxivity. They obtained surface relaxivity of 16 μm/s for a Fontainebleau sandstone. Fordham et al. (1994) obtained diffusion data at various diffusion times for a Clashach sandstone and then fitted them using Eq. 13 to estimate S/V. They obtained a surface relaxivity of 31 μm/s.

A sequence based on four-bipolar-gradients stimulated echo sequence, originally developed by Cotts et al. (1989), was used for diffusion measurements. This sequence was modified by applying a small-amplitude crusher gradient during the phase storage period (Figure 1) to dephase the signals from the extra echoes generated by multiple rf pulses (Chen et al., 1993b). The echo attenuation probed with this sequence is represented by

$$\frac{M(g_a,t)}{M(0)} = \exp[-\gamma^2 D(b_1 g_a^2 + b_2 g_0^2)], \tag{15}$$

where $M(0)$ contains the echo attenuation caused by relaxation and γ is the gyromagnetic ratio. The parameters g_a and g_0 are the applied and internal gradients, respectively. The time coefficients b_1 and b_2 are functions of experimental parameters.

A time-independent diffusivity is expected for a system without geometrical restriction, such as bulk fluid. Under these circumstances, the term related to g_0^2 is canceled when forming the ratio of echo amplitudes taken with a finite g_a and with $g_a = 0$:

$$\ln R = \ln\left[\frac{M(g_a,t)}{M(0,t)}\right] = -\gamma^2 D(b_1 g_a^2). \tag{16}$$

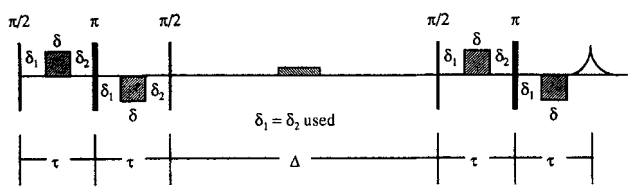

Figure 1. Four-bipolar-gradients stimulated echo sequence with a crusher gradient.

For geometrically restricted systems such as fluids confined in porous media, the diffusion echo attenuation can be expressed as the combination of two terms:

$$\ln R = \ln R_0 + \ln R_r. \tag{17}$$

The first term is the same as that for free diffusion:

$$\ln R_0 = -\gamma^2 D_0 (b_1 g_a^2). \tag{18}$$

The second term is the modification of echo attenuation because of the restricted diffusion effects (Chen et al., 1993b):

$$\ln R_r = D_0 \gamma^2 g_a^2 \frac{4}{9}\sqrt{\frac{D_0}{\pi}}\frac{S}{V}\left[\frac{8}{15}\delta(c_1^{2.5} - c_2^{2.5} - 2c_3^{2.5} + c_5^{2.5} - 2c_6^{2.5} - c_7^{2.5}) + \frac{16}{105}(c_2^{3.5} + c_3^{3.5} - c_4^{3.5} - c_1^{3.5} + c_5^{3.5} - c_6^{3.5} - c_7^{3.5} + c_8^{3.5})\right]. \tag{19}$$

The time coefficients c_i are determined from pulse sequence timing parameters. By varying the applied gradient g_a, a set of diffusion echo attenuation data $M(g_a,t)$ can be obtained. These data are used to estimate the pore volume-to-surface-area ratio V/S in Eq. 19. This parameter estimation problem can be solved by a linear least-squares algorithm. The use of this pulse sequence to estimate V/S from NMR diffusion measurements at short times is validated by analyzing certain model porous media with known V/S. Latour et al. (1993) used a different pulse sequence to estimate S/V of some glass bead packs.

Experiment

NMR experiments were performed with a GE 2-Tesla Omega CSI system operated at 85 MHz. The system is equipped with 20 gauss/cm gradient capability. A laboratory-built 4.45-cm-diameter birdcage rf coil was used in the experiments. The inversion-recovery pulse sequence and four-bipolar-gradients stimulated echo sequence with a crusher gradient were used for spin-lattice relaxation and diffusion measurements, respectively. Diffusion experiments were performed on glass bead packs and fully water-saturated rock samples to determine V/S. Spin-lattice relaxation experiments were performed on fully and partially water-saturated rock samples to determine $P(\tau_1)$. All measurements were performed at regulated room temperature.

The glass bead cleaning procedures described in Chen et al. (1992) were employed. The cleaned glass beads were then packed with deionized water inside glass vials with 10-mm ID and 28-mm height. Vibration and centrifuge methods were used to ensure close packing in the glass vials. No air bubbles were observed. Three different sized glass bead packs were used for diffusion experiments (Table 1). The pore volume-to-surface-area ratios of these bead packs can be estimated from the glass bead sizes d by

$$\frac{V}{S} = \frac{\sqrt{2} - \pi/3}{\pi} d \simeq 0.12\, d, \tag{20}$$

Table 1. Pore Volume-to-Surface-Area Ratios for Glass Bead Pack Samples Calculated by Eq. 20 and Estimated by NMR Diffusion Measurements

Sample	Glass Bead Size, d (μm)	V/S Calc. by Eq. 20 (μm)	V/S Est. by Diff. Exp. (μm)
Bead pack 1	1–38	0.12–4.56	4.47
Bead pack 2	90–125	10.8–15	13.0
Bead pack 3	125–180	15–21.6	14.5

which is based on the ideal packing model (Chen et al., 1992). This represents a rough estimate since there is a distribution of bead sizes, and they are not ideally packed. The values of bead sizes and pore volume-to-surface-area ratios calculated by Eq. 20 for the various bead packs are listed in Table 1.

Three cylindrical Bentheimer sandstone, Berea sandstone, and Texas Cream limestone samples, 2.54 cm in diameter and 3.25 cm in length, were used in the experiments. The values of porosity and permeability of these samples are listed in Table 2. These samples were saturated with deionized water. No significant weight change between the beginning and the end of the measurements was observed. A drainage device was designed to obtain uniform partial saturations (Chen et al., 1993a). Pressurized nitrogen gas was used to displace water.

Two chalk samples, BS2 and DU1, 2.54 cm in diameter and 2.54 cm in length, were also studied to compare the pore-size distributions obtained from NMR techniques with those from mercury porosimetry. These two samples and the values of their porosity and absolute permeability (see Table 2) were provided by RF-Rogaland Research, Stavanger, Norway.

Results and Discussion

The pore volume-to-surface-area ratios V/S of three glass bead pack samples were estimated from NMR diffusion measurements and are listed in Table 1 along with those calculated from Eq. 20. The V/S obtained from these two approaches seem quite consistent, particularly considering the approximate nature of Eq. 20. These results suggest that NMR diffusion measurements can provide a valid approach to estimate pore volume-to-surface-area ratios.

The method described previously was used to estimate $P(\tau_1)$ of rock samples at various water saturations. B-spline functions of order three were used. The procedure used to select the regularization parameter is illustrated with data of the fully water-saturated Texas Cream limestone sample. Equations 9 and 10 were solved with a number of different

Table 2. Certain Physical Properties of Rock Samples Studied in this Work

Sample	Porosity	Permeabilty (md)	Surface Relaxivity (μm/s)	V/S (μm)
Bentheimer	0.26	1,200	9.3	11.6
Berea	0.22	380	9.8	6.9
Texas Cream	0.24	17	7.1	3.5
BS2	0.28	7.6	23	2.9
DU1	0.47	9.4	23	3.2

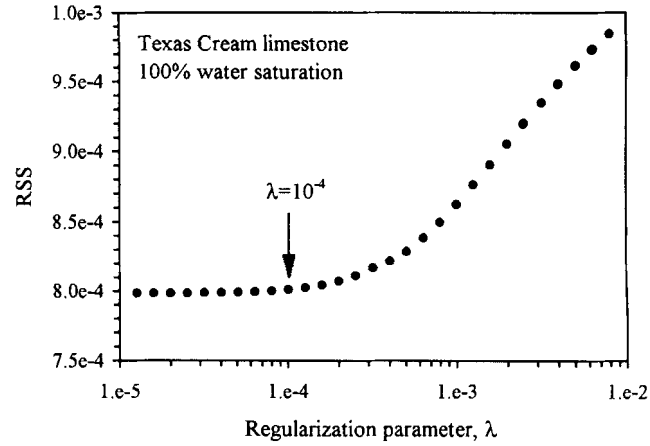

Figure 2. Residual sum of squares for different values of the regularization parameter, λ.

values of λ. The corresponding residual sum of squares (RSS $\equiv \|Y^{obs} - AC\|^2$) is plotted with λ in Figure 2. For relatively small values of the regularization parameter, all the major trends in the observed data have been reconciled by the corresponding calculated values, and the RSS reflects the level of experimental error. We have selected a value of 10^{-4} for the regularization parameter as the largest value that does not compromise the fit to the data. The function $P(\tau_1)$ corresponding to that value of the regularization parameter is our estimate of the distribution.

To convert $P(\tau_1)$ to $P(V/S)$, the information about surface relaxivity ρ is required. Surface relaxivity was evaluated by comparing V/S and average τ_1. The calculated values of V/S and ρ for these rock samples are listed in Table 2. The values of surface relaxivity obtained for Bentheimer and Berea sandstones are the same order of magnitude with that obtained by Kenyon et al. (1989) for Cherty sandstones (10 μm/s) using thin-section analysis. The values of surface relaxivity estimated for BS2 and DU1 are very close to each other, which is reasonable, considering that they have similar chemical compositions.

The pore-size distribution converted from $P(\tau_1)$ for a fully water-saturated Bentheimer sandstone is shown in Figure 3 with a semilog scale. To present the distribution curve in a fashion so that the area under an incremental part of the curve is directly proportional to the relative amount of fluid (or the percentage of pore volume for full water-saturation cases) associated with the corresponding pore volume-to-surface-area ratio interval, we adopted a convention that has been used to represent the pore-size distributions obtained from mercury porosimetry (Lowell and Shields, 1982). Instead of $P(V/S)$,

$$P[\log(V/S)] = P(V/S)\cdot\frac{V}{S} \tag{21}$$

is used in all of the figures to represent pore-size distributions or fluid distributions. The number located under each distribution peak represents the area corresponding to it. For Bentheimer sandstone, 79% of pore volume is associated with a pore volume-to-surface-area ratio interval ranging from

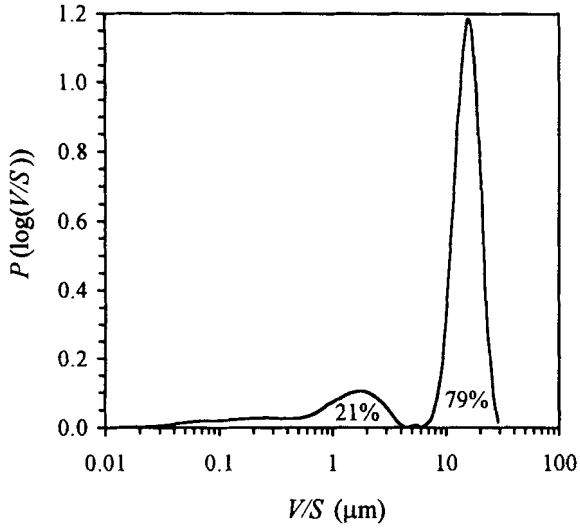

Figure 3. Pore-size distribution at full water saturation for a Bentheimer sandstone.

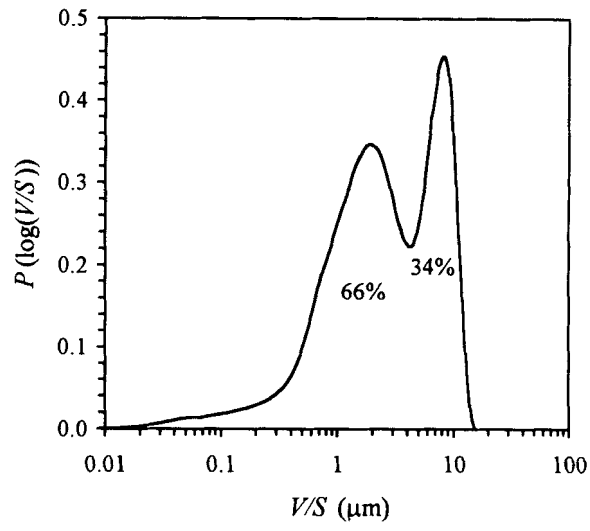

Figure 5. Pore-size distribution at full water saturation for a Texas Cream limestone.

about 6 to 30 μm; the remaining volume is associated with an interval from about 0.01 μm to 4 μm. We also had this Bentheimer sandstone tested by thin-section analysis and found that this sample has abundant primary intergranular pores and less abundant secondary pores. This is consistent with the observations from Figure 3.

The pore-size distribution of Berea sandstone is presented in Figure 4. Again, the number located under each distribution peak represents the area corresponding to it. It is found from thin-section analysis that the pore volume of this sample is dominated by the primary intergranular pores and the secondary pores are less common, which is also consistent with the observations from NMR pore-size distribution.

The pore-size distribution of Texas Cream limestone (Figure 5) is different from those of the sandstone samples. The primary intergranular pores do not dominate the pore volume of this sample, which is consistent with our results from thin-section analysis. The abundant secondary pores in the carbonate samples might account for the fact that the absolute permeability of this sample is much less than those of sandstone samples, while its porosity is not significantly less than that of Bentheimer sandstone sample and is even greater than that of the Berea sandstone sample (Table 2).

The $P[\log(V/S)]$ obtained from the Bentheimer sandstone at various water saturations, S_w, are multiplied by the corresponding saturations and then shown in Figure 6 with a semilog scale. The area under a selected segment of the $S_w * P[\log(V/S)]$ curve is proportional to the absolute water quantity confined in pores within the corresponding pore-size range. Therefore, Figure 6 actually represents the variations of fluid phase distributions in the two-fluid-phase systems as

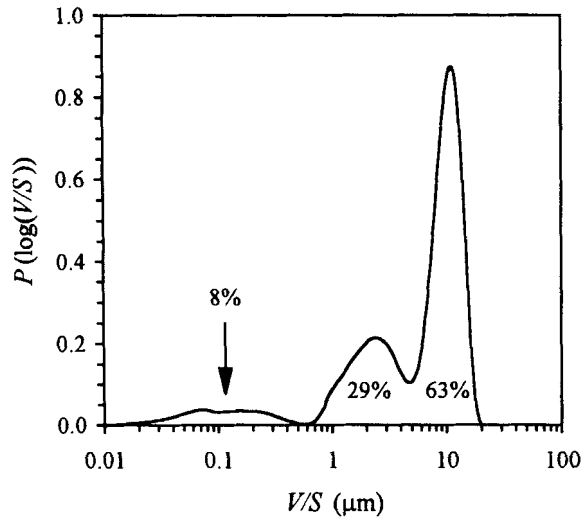

Figure 4. Pore-size distribution at full water saturation for a Berea sandstone.

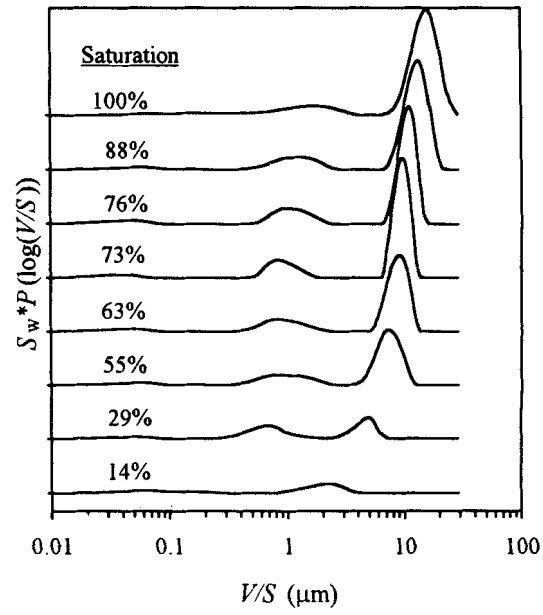

Figure 6. Fluid distributions in a Bentheimer sandstone at various water saturations.

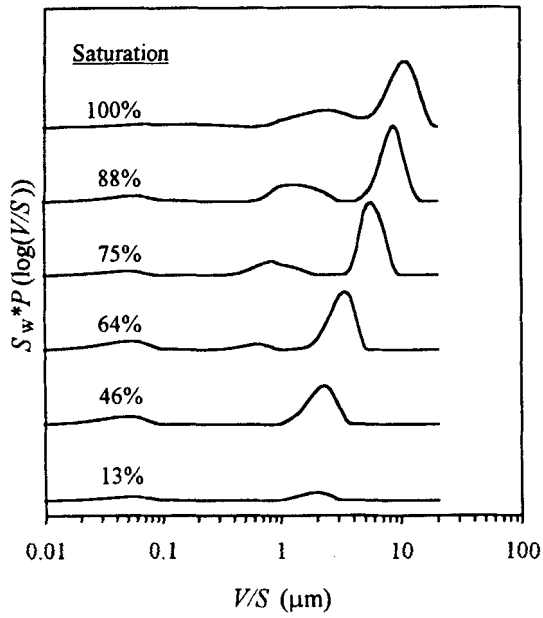

Figure 7. Fluid distributions in a Berea sandstone at various water saturations.

saturation is decreased. Those numbers located beside the fluid phase distribution curves represent the corresponding saturations. The area under the major peak (the peak at large V/S) decreases monotonically while S_w is decreased and the area under the minor peak does not change significantly until the lowest S_w is reached. This indicates that water was displaced from large pores at high saturation; while further decreasing the saturation, water in small pores was also displaced. These observed variations of fluid phase distributions are expected for the partially water-saturated samples prepared by drainage processes. An interesting phenomenon observed from Figure 6 is that the fluid distribution curve moves toward small V/S as S_w is decreased, which is probably due to some of the pores remaining partially filled with water as water was displaced out of the samples. Similar phenomena are also observed for the variations of fluid distributions in Berea sandstone (Figure 7) and Texas Cream limestone (Figure 8).

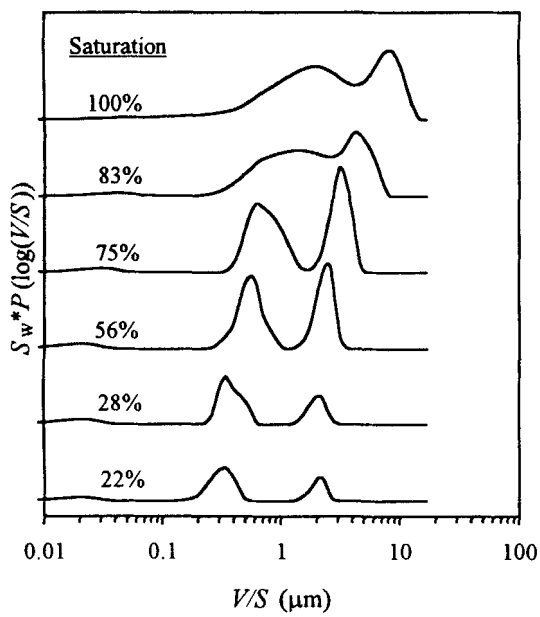

Figure 8. Fluid distributions in a Texas Cream limestone at various water saturations.

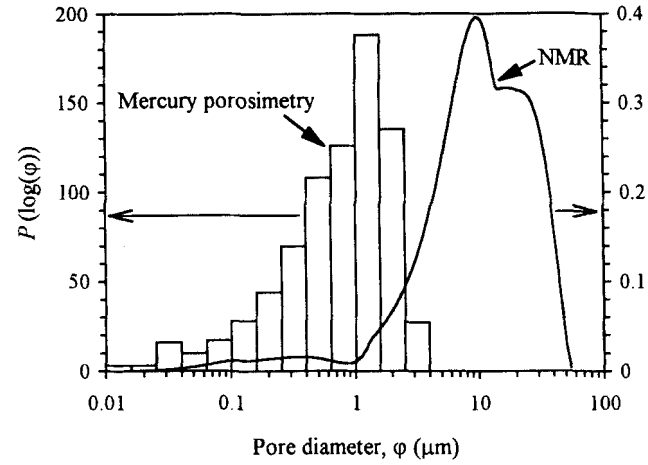

Figure 9. Pore-size distributions of a chalk sample, BS2, obtained by NMR techniques and mercury porosimetry, respectively.

The pore-size distributions of chalk samples, BS2 and DU1, obtained from NMR techniques are compared with those obtained from mercury porosimetry in Figures 9 and 10, respectively. The mercury porosimetry results were provided by RF-Rogaland Research. Since the mercury porosimetry and NMR pore-size distributions are presented in terms of pore diameter, φ, and pore volume-to-surface-area ratio, V/S, respectively, a certain pore-geometry assumption is required to make the comparisons. Assuming spherical pore geometry, $\varphi = 6(V/S)$. Since mercury porosimetry is based on the Washburn equation (Lowell and Shields, 1984), the results tend to reflect pore throats, instead of pore sizes. The NMR pore-size distributions demonstrated in Figures 9 and 10 are

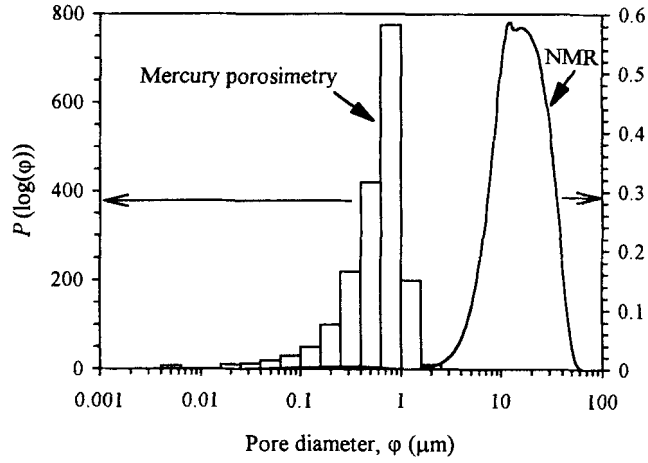

Figure 10. Pore-size distributions of a chalk sample, DU1, obtained by NMR techniques and mercury porosimetry, respectively.

about one order of magnitude greater than the corresponding mercury porosimetry pore-throat-size distributions, as expected. The patterns and peak widths of these two distributions are very similar to each other, although we would not necessarily expect this degree of similarity in general.

The fast-exchange limit requires that (Brownstein and Tarr, 1979)

$$\frac{\rho a}{D} \ll 1, \tag{22}$$

where a is the equivalent pore radius. If the pore geometry is assumed to be spherical ($V/S = a/3$) and the diffusivity of bulk water ($D \approx 2.5 \times 10^3$ $\mu m^2/s$) is used in the calculation, this relationship leads to

$$\frac{V}{S} \ll 100\ \mu m. \tag{23}$$

The maximum V/S observed for these rock samples is about 30 μm. Therefore, the fast-exchange limit is valid for the cases studied here.

The minimum pore size that can be estimated by this technique is determined from the minimum recovery time used in the experiments. Any signal corresponding to the water confined in small pores with relaxation time less than the minimum recovery time is insignificant to the experimental data. The minimum recovery time used for our experiments is 0.1 ms. The minimum τ_1 estimated is also about 0.1 ms. Therefore, the minimum recovery time used for these experiments is small enough to cover the entire pore-size distribution ranges of these samples. However, this would not necessarily be true if certain porous media with very small pores are studied. It is also noted that the neglect of interpore coupling might not be valid in small pores. The pore-size distributions for small pores might be associated with several even smaller pores lumped together by interpore diffusion of water molecules.

Conclusions

A new method has been developed for estimating pore-size and fluid phase distributions in porous media from NMR spin-lattice relaxation data. The relaxation time distribution functions are represented by B-splines, and Tikhonov regularization is used to stabilize the estimation problem. NMR restricted diffusion experiments are used to estimate the pore volume-to-surface-area ratios V/S of rock samples. This information is used in conjunction with relaxation time distributions to determine surface relaxivity. We have validated this method by analyzing certain model porous media with known V/S.

Pore-size distributions were estimated from data collected in samples that were fully saturated, and fluid phase distributions were estimated by measurements at different levels of fluid saturation. The pore-size ranges obtained from thin-section analyses are qualitatively consistent with the observations from our pore-size distributions. The observed variations of fluid phase distributions as saturation was decreased are consistent with those expected in a drainage process.

Acknowledgments

Partial support for this work was provided by the Office of the Vice President for Research and Associate Provost for Graduate Studies, through the Center for Energy and Mineral Resources, Texas A&M University. Financial assistance was also obtained from a University-Industry Cooperative Research Program for Petrophysical and Reservoir Engineering Applications of NMR at Texas A&M University. We also acknowledge RF-Rogaland Research for providing chalk samples with petrophysical information.

Notation

C = vector of B-spline parameters, dimensionless
d = glass bead size, μm
J = objective function, (digitizer unit)^2
M^{obs} = observed magnetization, digitizer unit
m = geometric factor
R = ratio of magnetizations, dimensionless
S = pore surface area, μm^2
V = pore volume, μm^3
Y^{cal} = the vector of calculated magnetizations, digitizer unit
Y^{obs} = the vector of observed magnetizations, digitizer unit

Greek letters

δ = gradient length, s
τ_{1min} = minimum τ_1 value for τ_1 distribution, s
τ_{1max} = maximum τ_1 value for τ_1 distribution, s

Literature Cited

Bard, Y., *Nonliner Parameter Estimation*, Academic Press, New York (1974).

Borgia, G. C., A. Brancolini, R. J. S. Brown, P. Fantazzini, and G. Ragazzini, "Water-Air Saturation Changes in Restricted Geometries Studied by Proton Relaxation," *Mag. Reson. Imag.*, **12**, 191 (1994).

Brown, J. A., L. F. Brown, J. A. Jackson, J. V. Milewski, and B. J. Travis, "NMR Logging Tool Development: Laboratory Studies of Tight Gas Sands and Artificial Porous Material," Unconventional Gas Recovery Symp., SPE/DOE paper 10813, Pittsburgh (May 16–18, 1982).

Brownstein, K. R., and C. E. Tarr, "Spin-Lattice Relaxation in a System Governed by Diffusion," *J. Mag. Reson.*, **26**, 17 (1977).

Brownstein, K. R., and C. E. Tarr, "Importance of Classical Diffusion in NMR Studies of Water in Biological Cells," *Phys. Rev. A*, **19**, 2446 (1979).

Chen, S., P. Miao, and A. T. Watson, "Characterization of Pore Structures Using NMR-Restricted Diffusion Measurements," SPE Technical Conf., paper 24812, Washington, DC (Oct. 4–7, 1992).

Chen, S., H.-K. Liaw, and A. T. Watson, "Saturation Dependent Nuclear Magnetic Resonance Spin-Lattice Relaxation in Porous Media and Pore Structure Analysis," *J. Appl. Phys.*, **74**, 1473 (1993a).

Chen, S., J. Qiao, H.-K. Liaw, and A. T. Watson, "Studies of Rock Structures Using NMR Restricted Diffusion Measurements and Analyses," *Proc. SCA Tech. Conf.*, paper 9313, Houston (Aug. 9–11, 1993b).

Chen, S., H.-K. Liaw, and A. T. Watson, "Measurement and Analysis of Fluid Saturation Dependent NMR Relaxation and Linebroadening in Porous Media," *Mag. Reson. Imag.*, **12**, 201 (1994).

Cotts, R. M., M. J. R. Hoch, T. Sun, and J. T. Markert, "Pulsed Field Gradient Stimulated Echo Methods for Improved NMR Diffusion Measurements in Heterogeneous Systems," *J. Mag. Reson.*, **83**, 252 (1989).

Fordham, E. J., S. J. Gibbs, and L. D. Hall, "Partially Restricted Diffusion in a Permeable Sandstone: Observations by Stimulated Echo PFG NMR," *Mag. Reson. Imag.*, **12**, 279 (1994).

Gallegos, D. P., and D. M. Smith, "A NMR Technique for the Analysis of Pore Structure: Determination of Continuous Pore Size Distributions," *J. Colloid Interface Sci.*, **122**, 143 (1988).

Groetsch, C. W., *The Theory of Tikhonov Regularization for Fredholm Equations of the First Kind*, Pitman, Boston (1984).

Hansen, P. C., "Analysis of Discrete Ill-Posed Problems by Means of the L-curve," *SIAM Rev.*, **34**, 561 (1992).
Haus, J. W., and K. W. Kehr, "Diffusion in Regular and Disordered Lattices," *Phys. Rep.*, **150**, 263 (1987).
Howard, J. J., and E. A. Spinler, "Nuclear Magnetic Resonance Measurements of Wettability and Fluid Saturations in Chalk," SPE Tech. Conf., paper 26471, Houston (Oct. 3–6, 1993).
Hürlimann, M. D., L. L. Latour, and C. H. Sotak, "Diffusion Measurement in Sandstone Core: NMR Determination of Surface-to-Volume Ratio and Surface Relaxivity," *Mag. Reson. Imag.*, **12**, 325 (1994).
Kenyon, W. E., J. J. Howard, A. Sezginer, C. Straley, A. Matteson, K. Horkowitz, and R. Ehrlich, "Pore-Size Distribution and NMR in Microporous Cherty Sandstones," SPWLA Logging Symp., Paper LL, New Orleans (June 11–14, 1989).
Latour, L. L., P. P. Mitra, R. L. Kleinberg, and C. H. Sotak, "Time-Dependent Diffusion Coefficient of Fluids in Porous Media as a Probe of Surface-to-Volume Ratio," *J. Mag. Reson.*, **101**, 342 (1993).
Lawson, C. L., and R. J. Hanson, *Solving Least Squares Problems*, Prentice-Hall, Englewood Cliffs, NJ (1974).
Lowell, S., and J. E. Shields, *Powder Surface Area and Porosity*, Chapman & Hall, New York (1984).
Merz, P. H., "Determination of Adsorption Energy Distribution by Regularization and a Characterization of Certain Adsorption Isotherms," *J. Comput. Phys.*, **38**, 64 (1980).
Mitra, P. P., and P. N. Sen, "Effects of Microgeometry and Surface Relaxation on NMR Pulsed-Field-Gradient Experiments: Simple Pore Geometries," *Phys. Rev. B*, **45**, 143 (1992).
Mitra, P. P., P. N. Sen, and L. M. Schwartz, "Short-Time Behavior of the Diffusion Coefficient as a Geometrical Probe of Porous Media," *Phys. Rev. B*, **47**, 8565 (1993).
Schumaker, L. L., *Spline Functions: Basic Theory*, Wiley, New York (1981).
Straley, C., C. E. Morriss, W. E. Kenyon, and J. J. Howard, "NMR in Partially Saturated Rocks: Laboratory Insights on Free Fluid Index and Comparison with Borehole Logs," SPWLA Logging Symp., Paper CC, Houston (June 16–19, 1991).
Wahba, G., "Practical Approximate Solutions to Linear Operator Equations When the Data are Noisy," *SIAM J. Numer. Anal.*, **14**, 651 (1977).
Whittall, K. P., M. J. Bronskill, and R. M. Henkelman, "Investigation of Analysis Techniques for Complicated NMR Relaxation Data," *J. Mag. Reson.*, **95**, 221 (1991).
Yang, P.-H., and A. T. Watson, "A Bayesian Methodology for Estimating Relative Permeability Curves," *SPE Reservoir Eng.*, **6**, 259 (1991).
Zimmerman, J. R., and W. E. Brittin, "Nuclear Magnetic Resonance Studies in Multiple Phase Systems: Lifetime of a Water Molecule in an Adsorbing Phase on Silica Gel," *J. Phys. Chem.*, **61**, 1328 (1957).

Manuscript received Oct. 6, 1994, and revision received Mar. 17, 1995.